Available online at www.sciencedirect.com

ScienceDirect

Mendeleev Commun., 2023, **33**, 433–435

Mendeleev Communications

Modes of interaction of counterflow flames in diluted methane–oxygen mixtures in a closed reactor

Nikolai M. Rubtsov,*[a] Victor I. Chernysh,[a] Georgii I. Tsvetkov[a] and Kirill Ya. Troshin[b]

[a] *A. G. Merzhanov Institute of Structural Macrokinetics and Materials Science, Russian Academy of Sciences, 142432 Chernogolovka, Moscow Region, Russian Federation. Fax: +7 495 962 8025; e-mail: nmrubtss@mail.ru*

[b] *N. N. Semenov Federal Research Center for Chemical Physics, Russian Academy of Sciences, 119991 Moscow, Russian Federation*

DOI: 10.1016/j.mencom.2023.04.043

The features of the interaction of counterflow flames in diluted methane–oxygen mixtures at a total pressure of up to 200 Torr in a closed reactor were established. It was found that in the mode of interaction of flames propagating in hot reaction products, two-dimensional flame vortices arise due to density stratification; flames, propagating through the initial mixture, interact with the formation of only three-dimensional structures.

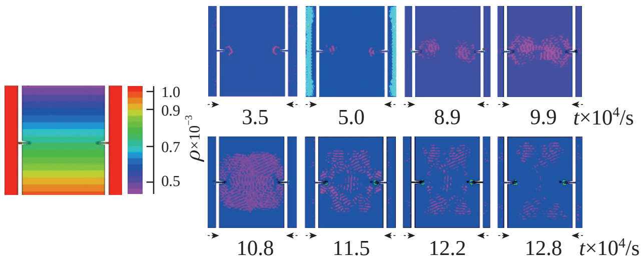

Keywords: combustion, methane, counterflow, vortex, kinetic, gas dynamics.

Counterflow flames provide a unique platform for understanding the interactions between mixing processes and chemical reaction kinetics and can serve as a model for studying the effects of physical and chemical perturbations on flame structure using axially opposed symmetric flame jets.[1–3] It should be noted that even in the absence of chemical reactions, the instabilities arising from the interaction of counter jets are poorly understood. The literature provides data on the interaction of coaxial counterflows of liquids, demonstrating the occurrence of various vortex structures.[4]

In the following, we used the terminology given in the published work:[3] counterflow flames are twin flames generated by two identical opposing jets of fuel–air mixtures (two identical, axisymmetric, premixed jets of reactants shooting into each other).

It is well-known that vortices are characteristic features in large-scale geophysical flow systems. In particular, it became clear from satellite imagery that the Earth's atmosphere and its oceans contain a wealth of horizontal structures in a range of spatial scales, such as large-scale vortices, which usually have a long lifetime. A common feature of these vortices is that their flow field is almost two-dimensional. The analysis carried out in previous works[5–7] showed that in a density-stratified medium, the initially three-dimensional isotropic turbulence forms quasi-two-dimensional vortex rings (hereinafter, 2D vortices). Density stratification can be caused by temperature gradients or differences in the concentration of the starting reactant or intermediate. Energy sources for this can be found in decaying convective clouds and thunderstorm anvil outflows. The role of these phenomena in reactive flows has not been sufficiently determined.

As shown in the cited paper,[8] the propagation of counterflow flames caused by simultaneous initiation at opposite butt-ends of a cylindrical reactor leads to a significantly greater increase in pressure (by a factor of ~2) than in the case of flame propagation from a single initiating source. This indicates the importance of identifying the patterns of flame propagation initiated by two or more ignition sources for explosion safety problems. As was shown earlier,[9] flame fronts (including counterflow flames) in mixtures of H_2 and CH_4 with oxygen in closed cylindrical vessels propagate with variable velocities; in addition, the transition from a spherical flame arising upon initiation to propagation in a cylindrical pipe is accompanied by the appearance of instabilities at the flame front.

Previously, we have shown[10,11] that the ignition of a methane–oxygen mixture (total pressure up to 200 Torr) behind a single obstacle with a small circular opening is observed at a noticeable distance from the surface of the obstacle ('flame jump'). 'Flame jump' is the distance the flame front occurs behind the obstacle. It was shown that the length of the 'flame jump' after the opening in the obstacle is mostly determined by the time of the transition from laminar to turbulent flow, rather than by the ignition delay time. Thus, the relative contribution of gas-dynamic factors to the process is essentially higher than that of kinetic ones.

This work is aimed at revealing, by means of high-speed filming, the interaction modes of flames propagation in hot reaction products and in the initial gas mixture in a closed cylindrical reactor after spark initiation and qualitative interpretation of these modes using numerical calculations.

First, the interaction of flame jets of the initial mixture in hot combustion products was investigated. The temperature in the flames interaction zone was estimated. For the readings of the flame pyrometer, the value $\varepsilon = 0.1$ was chosen.[12] The values measured by two methods are in satisfactory agreement, giving 1020 °C, but they obviously represent the lower limit of the real value. Figure 1 shows the results of high-speed filming of the outflow of a flame jet from one compressible syringe (the second syringe was plugged) at an initial pressure of 180 Torr. As seen in Figure 1, the hot products of the propagating flame cause the syringe to compress and a gas jet to emerge from its nozzle; the jet ignited in the hot gas forms a 2D vortex in a horisontal plane, observed in a side view [Figure 1(*a*)], *i.e.*, the fact that gas-dynamic vortices spread in a combustible environment made it possible to visualize these vortices. In our experiments, there were deviations

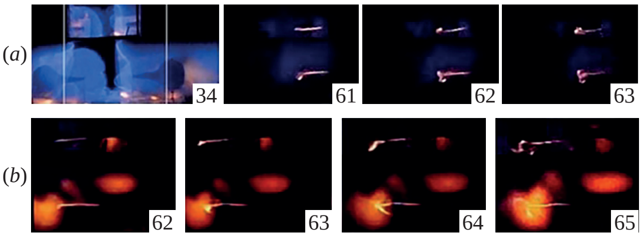

Figure 1 High-speed filming of the emergence of two-dimensional vortex rings from flame jets generated by a single compressible syringe in hot reaction products. (*a*),(*b*) Frames from two separate experiments. Initial pressure, 180 Torr. The figures on each frame correspond to the frame number after an initiating discharge.

of the vortices [Figure 1(*b*)] from the horizontal plane, related to the deviation in the direction of density stratification caused by temperature gradients arising in the random process of flame turbulence decay [see Figure 1(*a*), frame 34].

Figure 2 shows typical results of high-speed filming of the interaction of counter flame jet outflows from the compressible syringes at an initial pressure of 180 Torr. As can be seen in Figure 2(*b*),(*d*), the hot products of the propagating flames cause the compression of the syringes and the emergence of gas jets from their nozzles; the jets then ignite in the hot gas, forming counterflow flame fronts. The interaction of counterflow flames is accompanied by the formation of vortices; the behavior of the vortices is not the same in different experiments, and also varies depending on the orientation of the density stratification caused by temperature gradients that arise in the random process of flame turbulence decay, as was demonstrated above in Figure 1.

We have observed two types of interaction of counter jets, corresponding to the interaction of jets in a gas in which either density stratification has already occurred [see Figure 2(*b*)] or

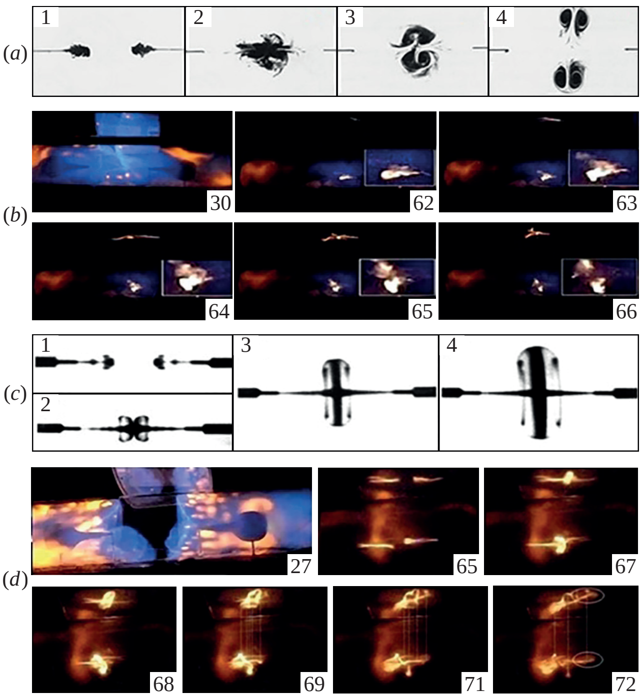

Figure 2 Sequences of side view photographs showing (*a*) the collision of two jets with the same momentum and the formation of a vortex quadrupole in a linearly stratified fluid, and (*c*) the frontal collision of two round jets in an experiment with distilled water as a fluid and the formation of a toroidal vortex ring-like structure. (*b*),(*d*) High-speed filming of the interaction of counter flame jets generated by compressible syringes in two separate experiments. Initial pressure, 180 Torr. The figures on each frame correspond to the frame number after an initiating discharge, the ellipses indicate two-dimensional dipolar vortices, and the white lines correspond to the same time.

the gas density at the moment of interaction is relatively uniform [see Figure 2(*d*)]. Figure 2(*a*)[13] and Figure 2(*c*)[4] illustrate the features of the interaction of jets in liquids observed in earlier works. Notice that the density uniformity [see Figure 2(*d*)] can be maintained only at the moment of jet interaction, after which the toroidal flame vortex falls apart [see Figure 2(*d*), frames 68–71]. The resulting density stratification is evidenced by the formation of a 2D flame vortex [see Figure 2(*d*), frame 72]. Therefore, under conditions of nonuniform density stratification, 2D flame vortices can propagate out of the zone of counter jets interaction. This is important for explosion safety problems, because 2D flame vortices can penetrate through narrow gaps, which can be present in manufacturing facilities.

As follows from the discussion above, the analysis of gas-dynamic factors is sufficient for a qualitative consideration of the observed features. In Figure 3,[16] the interaction of counter jets is illustrated by the results obtained by the finite element analysis using the FlexPDE 6.08 software package (PDE Solutions Inc., 1996–2008, example 2D_PISTON_MOVINGMESH.PDE).[14] A 2D flow of an ideal gas in a compressor cylinder was modeled in cylindrical (r, z) coordinates [Figure 3(*a*)]. The initial gas pressure is chosen to be 100 Torr. The domain boundaries move according to the movement of the counter pistons, while the interior mesh is tensioned within the moving boundaries. This results in a fixed Lagrangian–Eulerian model in which the mesh moves but with different velocity than the gas:

$$\frac{\partial \rho}{\partial t} + \left(\frac{\partial \rho u r}{\partial r}\right)/r + \frac{\partial \rho v}{\partial z} = C_1 \mathrm{div}(\mathrm{grad}(\rho)), \quad (1)$$

$$\frac{\partial u}{\partial t} + u\frac{\partial u}{\partial r} + v\frac{\partial u}{\partial z} + \frac{\partial P}{\partial r}/\rho = C_2 \mathrm{div}(\mathrm{grad}(u)) - C_2 u/r^2, \quad (2)$$

$$\frac{\partial v}{\partial t} + u\frac{\partial v}{\partial r} + v\frac{\partial v}{\partial z} + \frac{\partial P}{\partial z}/\rho = C_2 \mathrm{div}(\mathrm{grad}(v)), \quad (3)$$

$$\frac{\partial P}{\partial t} + u\frac{\partial P}{\partial r} + v\frac{\partial P}{\partial z} + \gamma P\left(\frac{\partial r u}{\partial r}/r + \frac{\partial v}{\partial z}\right) = C_1 \mathrm{div}(\mathrm{grad}(P)). \quad (4)$$

Here C_1 is the smoothing coefficient: $C_1 = \mathrm{sqrt}(\gamma P_0/\rho_0)$ $(R/\text{mesh grid})$, $C_2 = \max(\nu, C_1)$, t is the time, ρ and ρ_0 are the current and initial gas density, respectively, ν is the gas kinematic viscosity, u and v are the velocity components, P and P_0 are the current and initial pressure, respectively, $\gamma = 1.4$ is the ratio of specific heat capacities, and the boundary conditions are given in the cited book.[14] As seen in Figure 3, the calculations of vorticity $\omega = 1/2\,|\partial v/\partial z - \partial u/\partial r|$ acceptably illustrate the occurrence of two vortices in the direction perpendicular to the initial interacting counter jets.

Obviously, the description of such features as the observed decay of the toroidal vortex during the interaction of the initial jets and the subsequent appearance of a two-dimensional vortex

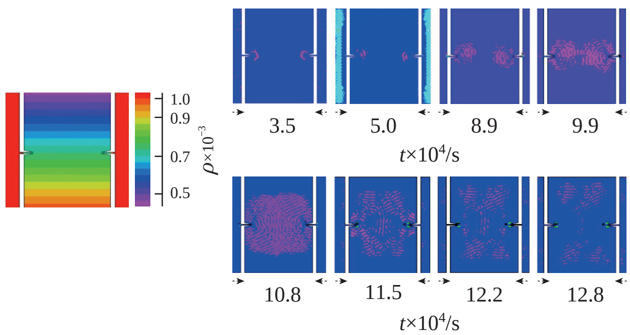

Figure 3 The results of calculating the vorticity ω in the process of interaction of counter non-reacting jets according to the mixed Lagrangian–Eulerian model, in which the mesh moves, but with different velocity than the gas. The domain boundaries move according to the left and right pistons, while the interior mesh is tensioned within the moving boundaries. On the left, the initial density stratification and density scale are shown. Arrows indicate the direction of boundaries movement.

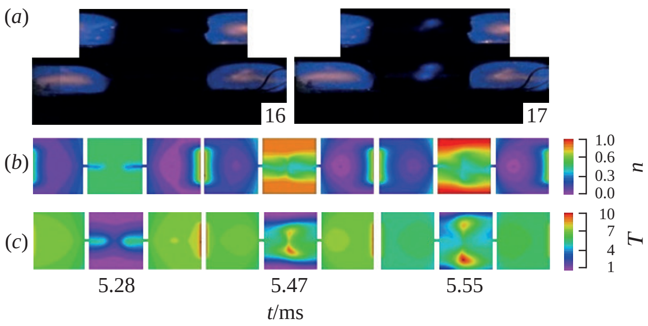

Figure 4 (*a*) Typical frame sequence of the interaction of counterflow flames penetrating through planar obstacles with central round openings. Initial pressure, 170 Torr. The figures on each frame correspond to the frame number after an initiating discharge. Results of the process calculation: (*b*) change in the dimensionless concentration *n* of the active intermediate and (*c*) change in the dimensionless temperature *T*. The scales of *n* and *T* are shown on the right.

due to density stratification requires 3D modeling. In addition, analyzing the problem of the interaction of combustible submerged jets under conditions of density stratification caused by temperature gradients arising in the random process of flame turbulence decay is of interest for solving explosion safety problems.

In another series of experiments, the interaction of submerged hot jets of the initial mixture in the environment of a cold initial gas was studied. The outcome of this experiment on the interaction of counterflow flames is shown in Figure 4(*a*). Thin obstacles with round central openings (30 mm in diameter) were placed opposite each other vertically in the center of the reactor. It should be noted that the size of the hole is limited by its smallest diameter, which under our conditions is 20 mm: the flame does not penetrate through a hole of a smaller diameter. The obstacles were placed at a distance equal to twice the 'flame jump' from each other, so that the flame front had time to emerge[9] for both opposite flows. Under our conditions, this distance was ~220 mm. Figure 4(*a*) shows a typical high-speed video frame sequence of a counterflow flame interaction.

As was shown in the cited work,[10] any comparison of the experimentally recorded movement of the flame emission front with the result of numerical modeling is credible only in qualitative aspects, such as changes in the velocity of the moving boundary of the initial actively reacting gas, the shape of this boundary, the degree of its 'smoothness' and pertubations of its structure. Thus, the reaction rate was presented without specifying the details of the chain mechanism. The set of compressible dimensionless reactive 2D Navier–Stokes equations in cylindrical coordinates[15] in the low Mach number approximation[9–11,16] was applied to illustrate the experimental results. In the model, the movement of gas and the appearance of jets were caused by the movement of counter combustion fronts. The process of chemical transformation was described by a simple chain mechanism.[10] The initiation condition was assumed to be $T = 10$ at the right and left boundaries of the channel; the channel had two orifices at the same distance from the butt-ends. The boundary conditions (including the orifices) were $C_\xi = 0$, $u = 0$, $v = 0$, $\rho_\xi = 0$, $n_\xi = 0$, as well as convective heat exchange $T_t = T - T_0$, where ξ is a dimensionless coordinate.

The results of qualitative calculations of the flame interaction are presented in Figure 4(*b*), which shows the change in the dimensionless concentration of the reagent, and in Figure 4(*c*), which shows the change in the dimensionless temperature. As can be seen, the results of the analysis are in qualitative agreement with the experimental data presented in Figure 4(*a*). Thus, the process has the characteristic time of a chemical reaction, and not a gas-dynamic one (*cf.* Figure 2 and Figure 4).

In addition, the resulting flame structures formed during the interaction of the flames have a 3D appearance, as can be seen in frame 17 in Figure 4(*a*). This is due to the actual absence of density stratification under the experimental conditions. This means that the relative contributions of gas-dynamic processes and chemical kinetics of the combustion reaction differ from the case of the interaction of flame jets of the initial mixture in hot combustion products. In this case, the analysis of a three-dimensional model is quite urgent for describing the regularities of the counterflow flames propagation in closed pipes. At the same time, the illustrative results of qualitative two-dimensional modeling taking into account gas-dynamic and kinetic factors, which are consistent with the results of our experiments, allow us to indicate further ways to modify three-dimensional analysis.

In summary, the features of the interaction of counterflow flames of diluted methane–oxygen mixtures at a total pressure of up to 200 Torr in a closed reactor were revealed. It was found that in the mode of interaction of flames propagating in hot reaction products, two-dimensional vortices arise due to density stratification. Under conditions of nonuniform density stratification, two-dimensional vortices can propagate far beyond the zone of counter jets interaction. It was also shown that counterflow flames propagating through the initial mixture interact with the formation of only three-dimensional structures.

Online Supplementary Materials

Supplementary data associated with this article can be found in the online version at doi: 10.1016/j.mencom.2023.04.043.

References

1 V. P. Gulakhe and R. B. Yarasu, *International Journal of Science Technology and Engineering*, 2015, **1** (12), 62.
2 J. M. A. Jaff, M. H. Tahir, Y. F. Tahir, S. S. Sleman and H. B. Abdullah, *IOSR Journal of Mechanical and Civil Engineering (IOSR-JMCE)*, 2015, **12** (6), 14.
3 A. G. Iyer, *PhD Thesis*, Technische Universiteit Eindhoven, 2018.
4 S. I. Voropayev, Y. D. Afanasyev, V. N. Korabel and I. A. Filippov, *Phys. Fluids*, 2003, **15**, 3429.
5 M. Beckers, *PhD Thesis*, Technische Universiteit Eindhoven, 1999.
6 V. V. Meleshko, A. A. Gourjii and T. S. Krasnopolskaya, *Journal of Mathematical Sciences*, 2012, **187**, 772 [*Matematychni Metody ta Fizyko-Mekhanichni Polya*, 2011, **54** (4), 184].
7 R. McKeown, R. Ostilla-Mónico, A. Pumir, M. P. Brenner and S. M. Rubinstein, *Physical Review Fluids*, 2018, **3**, 124702.
8 I. M. Naboko, N. M. Rubtsov, B. S. Seplyarskii, V. I. Chernysh and G. I. Tsvetkov, *Mendeleev Commun.*, 2013, **23**, 163.
9 N. M. Rubtsov, B. S. Seplyarskii, I. M. Naboko, V. I. Chernysh, G. I. Tsvetkov and K. Ya. Troshin, *Mendeleev Commun.*, 2014, **24**, 308.
10 N. M. Rubtsov, *Key Factors of Combustion: From Kinetics to Gas Dynamics*, Springer, Cham, Switzerland, 2017.
11 N. M. Rubtsov, V. I. Chernysh, G. I. Tsvetkov and K. Ya. Troshin, *Mendeleev Commun.*, 2019, **29**, 108.
12 J. Lin, X. Zhang, K. Liu and W. Zhang, *Energies*, 2019, **12**, 2185.
13 S. I. Voropaev and Ya. D. Afanasyev, *J. Fluid Mech.*, 1992, **236**, 665.
14 G. Backstrom, *Simple Fields of Physics by Finite Element Analysis*, GB Publishing, Malmö, Sweden, 2005.
15 N. M. Rubtsov, V. I. Chernysh, G. I. Tsvetkov and K. Ya. Troshin, *FirePhysChem*, 2021, **1**, 174.
16 A. Majda, *Compressible Fluid Flow and Systems of Conservation Laws in Several Space Variables*, Springer Science+Business Media, New York, 1984.

Received: 3rd November 2022; Com. 22/7040